Chapter 9

Performance Evaluation of a Probe Climber for Maintaining Wire Rope

In recent years, with barrier-free public facilities, elevators have come to be installed in stations and on footbridges. The shortage of maintenance technicians has become a social problem with the increase in elevator. In addition, an inspection of the elevator and the amusement machine that have been suspended by wire rope is often overlooked since it depends on visual inspection. For such a problem, by making a self-driving probe climber work efficiently, the safety of workers and an improvement in the quality of maintenance can be expected. In this chapter, we developed a self-driving probe climber to detect the wear and corrosion damage of the wire rope at an early stage. It also provides the results of their verification for damage detection performance of wire rope and driving performance.

9.1. Introduction

As public facilities have become barrier-free in recent years, elevators have been introduced in low-rise buildings, in station buildings and on pedestrian bridges, and the amount of elevator maintenance is approaching one million units. However, a shortage of engineers who possess proper maintenance techniques has become an issue. In addition, visual inspections are mostly conducted for double-track normal ropeway stays as well as

---

Chapter written by Akihisa TABATA, Emiko HARA and Yoshio AOKI.

amusement facilities for which fixed wire ropes are used for load bearing. Many of those maintenance inspections involve risks, such as high-place work. A countermeasure against these is to develop an automatic running inspection device having a function of early dection of the wire breakages, environmental degradation and abnormal abrasion of wire rope, by which secured safety of workers, streamlined inspection work and improved quality in maintenance inspections can be expected.

In this study, in order to develop a remote maintenance inspection system of wire rope for structures, an inspection device was first mounted for evaluating structural integrity and an elevation mechanism (probe climber) was fabricated that was capable of even vertical automatic movements. Then, through wire rope elevation experiments, appropriate conditions for friction drive to enable stable elevation with less energy consumption were examined. Magnetic flux leakage (MFL) flaw detect method is currently common for evaluating wire rope integrity. However, the method has limitations, such as the inspection device's scanning speed and detection accuracy for wire breakages and corrosion in rope trough and bottom areas has become an issue. This study considers the detection accuracy after configuring a sensor system of phased-array type Hall elements, which is more compact and accurate in detection than conventional products. It also describes the evaluation results through experiments for identifying the locations of damage/corrosion in conjunction with a drive control system of the automatic elevation device and makes a case analysis of damage/corrosion patterns by using cognition and judgment techniques.

9.2. Optimize friction drive conditions using a prototype probe climber

Figure 9.1 shows an automatic probe climber made as the first prototype. The designed probe climber has an elevation mechanism where a wire rope is sandwiched between drive wheel and idler wheel, the latter of which is pressed against the wire rope in order to secure sufficient frictional force required to elevate the machine body. As shown in Figure 9.2, push mechanisms with screws and springs were fabricated for adjusting the pushing force of the idler wheel, and the impact of the adjustment made on the elevation performance and power consumption was examined [HAL 12].

The pushing force was adjusted relative to the total weight of the climber, in the range from the lower limit for securing the minimum frictional force required for vertical elevation to the upper limit at which elevation is no longer possible due to the high load of the pushing force. In the case of the

push mechanism with screws, the screws were tightened for each pitch, whose axial force was measured and managed by a load cell. For the push mechanism with springs, frictional force adjustment was made possible by retrofitting springs with different spring constants.

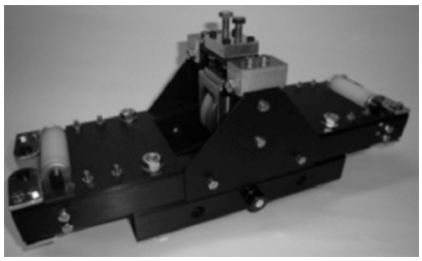

Figure 9.1. *Prototype model of prove climber*

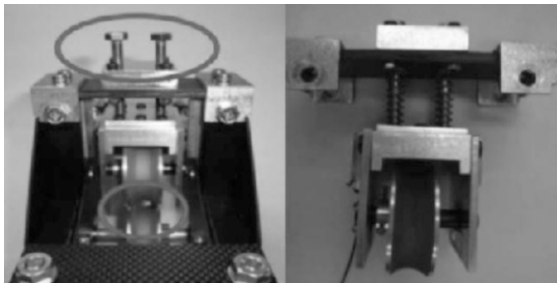

a) *Screws* *b*) *Springs*

Figure 9.2. *Friction force adjustment mechanism*

During the elevation experiments, the pushing forces were changed: 68.2 N (lower limit), 76.9, 85.6, 89.8, 93.9, 97.5 N (upper limit). Measurements were made for elevation speed, power consumption, three-axis acceleration and the rotational speed of drive shaft and idler shaft. Besides, the slip ratio of the drive wheel was calculated by the following formula:

$$S = \frac{v_w - v_v}{v_w} \qquad [9.1]$$

where S[%] is slip ratio, v_w is drive wheel speed and v_v is idler wheel speed. Table 9.1 and Figure 9.3 show the relationship between the slip ratio calculated by formula [9.1] and the pushing force.

	Screw				Spring			
Pushing force (N)	Slip ratio (%)	Current (A)	Time (s)	Vibration (m/s^2)	Slip ratio (%)	Current (A)	Time (s)	Vibration (m/s^2)
68.2	59	5.28	9.8	2.218	22	5.40	10.7	1.874
76.9	37	5.49	9.8	2.241	5	5.48	9.6	1.795
85.6	31	5.66	10.2	2.315	4	5.50	12.3	2.253
89.8	18	5.71	11.0	2.301	22	5.58	12.5	2.275
93.9	20	5.87	10.9	2.223	20	5.68	12.6	2.270
97.5	4	5.99	11.6	2.520	12	5.68	13.3	2.790

Table 9.1. *Climbing performance*

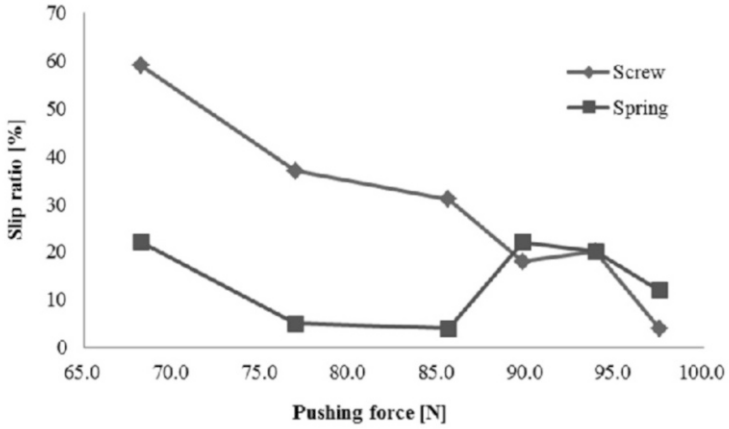

Figure 9.3. *Change of the slip rate with the pushing force*

It was found that in both mechanisms, the slip ratio would decrease, when the pushing force was increased from 68.2 to 85.6 N. The tendency showed that when the push mechanism with springs was adopted, its slip ratio would become smaller than that of the one with screws. Conceivably, the slip ratio became bigger in the screw pushing mechanism, where the idler wheel range of motion (ROM) is smaller than that in the spring pushing mechanism, thus the former could not follow changes in the wire rope diameter during the elevation. The vibration magnitude and the slip ratio in Table 9.1 indicated that even the spring pushing mechanism would have similar slip ratio to the screw pushing mechanism's, when the springs were compressed in the vicinity of the closed length. Furthermore, in the case of smaller pushing force, the spring pushing mechanism has a smaller vibration than the screw

pushing mechanism, thus vibration suppression effect can be expected when ROM is sufficiently secured in the spring pushing mechanism. Partly because the wire rope diameters in damaged and worn areas have locally changed, the probe climber should be designed so that the spring pushing mechanism may be proper with the spring ROM sufficiently secured.

9.3. Impact of different surface friction materials for friction pulley made on elevation performance

Consideration was made for inserting friction material onto the surface of the drive wheel and the idler wheel in order to cause no damage to the rope surface during wire rope maintenance inspection and ensure improvement in elevation performance. In this regard, a simple friction measuring device was made so as to measure coefficients of kinetic friction (μ) of various types of friction materials shown in Table 9.2, when they were pressed against a synthetic belt. Figure 9.4 shows the relationship between the pushing force and coefficients of kinetic friction. It was found that polychloroprene rubber among the friction material types is a suitable friction material with a relatively large kinetic friction coefficient, even though the hardness is 70. Also, the kinetic friction coefficient (μ) in any of the material types would be smaller, as the pushing force increased [SHA 12]. It has been verified that increased pushing force will add running load to the climber and increase energy consumption. Therefore, based on these findings, for designing a probe climber, it is necessary to make further considerations on how to secure a proper frictional force and reduce slips between the drive wheel and the wire rope without increasing the pushing force between the wheels and the rope.

Roller material	Hardness
Polychloroprene (CR)	70–90
Nitrile rubber (NBR)	
Polyurethane rubber (UR)	

Table 9.2. *Rubber materials for friction wheel*

Then, impact on power consumption was verified when the pushing force of the idler wheel was changed. Figure 9.5 shows the case of the screw pushing mechanism, where the time history of power consumption, measured during elevation with the pushing force changed in three patterns: 68.2 N, 85.6 N and 97.5 N, indicates that power consumption during elevation

increased in accordance with the pushing force increase. A possible reason for unstable power consumption shown in Figure 9.5 is the effect of the wire rope vibrated by the ropes unevenness and the wind.

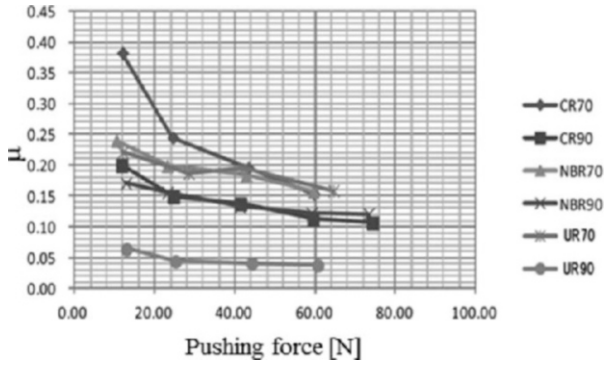

Figure 9.4. *Change of the friction coefficient with the pushing force*

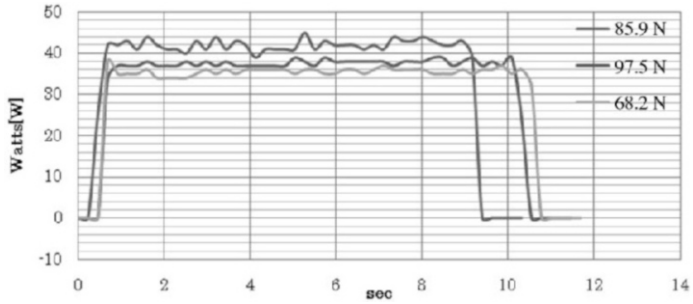

Figure 9.5. *Pushing force and Power consumption*

Based on the above measurement results, an improved probe climber was fabricated and shown in Figure 9.6 and the basic performance in Table 9.3. The improved probe climber was cable of stable elevation, because a bilateral symmetry layout was thoroughly ensured with multiple drive mechanisms and consideration was given to setting the center of the climber's gravity near the rope. Along with these, multiple drive wheels were used in order that the overall drive mechanism could reduce slips with the rope and vibrations. Also for the corresponding idler drive, the cross-section of the rope contact area was provided with a recess made of chloroprene material. In addition, the idler pulley shown in Figure 9.6, whose ball screw mechanism enables

position adjustment, makes it possible to adjust the contact area with the drive mechanism, depending on the wire rope tension. Furthermore, the climber is equipped with the function of regenerating potential energy by incorporating a power generating motor in place of a braking device used while an elevator lowers. Besides, as a countermeasure against regenerative mechanism failures, a ratchet mechanism shown in Figure 9.7 is also incorporated in order to prevent falling.

Additionally, an Xbee module and a directional antenna were used for communicating with the probe climber and it was verified that data communication with more than a 600 m distance was available. For the actual elevation experiments, in addition to monitoring the motor current, the voltage, the number of revolutions, a temperature sensor, an atmospheric pressure sensor, a humidity sensor, an acceleration sensor and a charge coupled devices (CCD) camera shown in Figure 9.8 were mounted.

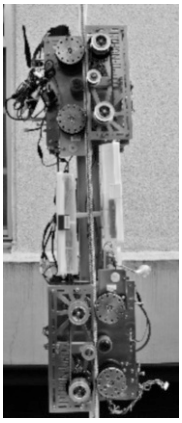

Figure 9.6. *Refined probe climber*

Length	1.2 (m)
Weight	9.5 (kg)
Number of motor	2
Maximum power of motor	2,900 (W)
Rotational Speed	247 (rpm/V)
Number of drive wheel	4
Maximum velocity	14 (m/s)

Table 9.3. *Technical specifications of refined probe climber*

Figure 9.7. *Ratchet brake*

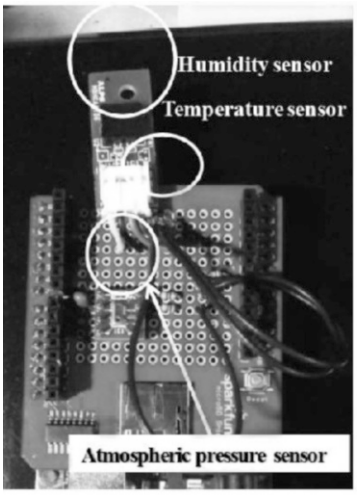

Figure 9.8. *Environmental sensor*

9.4. Damage detection test of elevator wire rope

Steel wire rope used for an elevator comprises of congregated twisted wires (called strands) made into a plurality of congregated twisted strands, with the fiber core as the axis. This is called a wire rope with *n* strands. Typically, 6–8 *n* strands are used for an elevator. In the damage detection test, as shown on the right side of Figure 9.10(b), 24 wires with 0.6 mm diameter was made into one strand. Wire rope made of six twisted strands was used, assuming the specimen wire rope with a cut in it (Figure 9.9(a))

have become loose and making use of two damage specimens in which wires as short as 10 mm were embedded (Figure 9.9(b)).

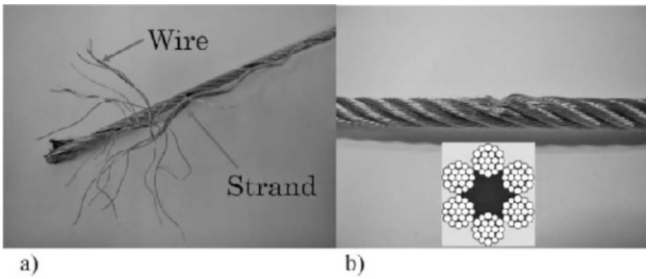

Figure 9.9. *Damaged steel wire rope*

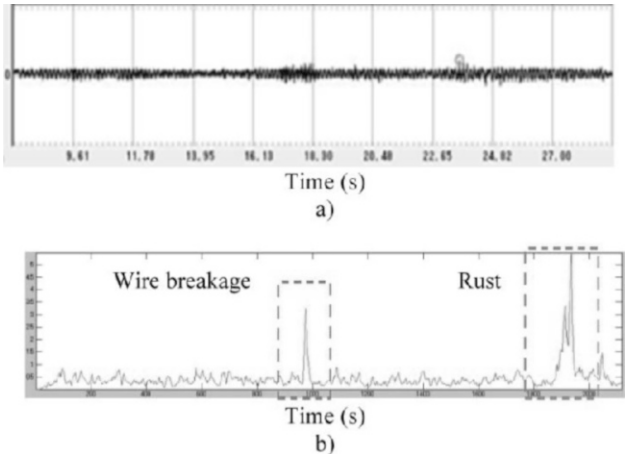

Figure 9.10. *Time history of a) the response vibration and b) the leakage flux*

First, the probe climber was used to take measurements with a wire rope tester for variations of response acceleration caused by damage to the wire rope and MFL caused by scratches and rust. Signal processing was performed on such measurement data to check the presence/absence of an abnormality judgment. The two signal processing methods were used: discrete Fourier transform (DFT) was used to analyze the power spectrum of each frequency and wavelet transform to express waveforms by scaling and shifting short waveforms called mother wavelets. Figure 9.10(a) shows the measurement results of response acceleration and Figure 9.10(b) shows that of MFL

strength. From the response acceleration measurement data (the original waveform), it is difficult to directly detect wire breakages and loosening, but from the MFL strength data, a clear change in the spectrum can be observed even in areas where wire breakages and rust have occurred.

9.5. Damage detection through signal processing

With the original waveform of the response acceleration in Figure 9.10(a), it is difficult to identify the presence or absence of damage and the location of damage. Thus, the two types of signal processing techniques were used to investigate the possibility of wire rope damage detection through response acceleration. First, frequency analysis was performed by applying the DTF to the original waveform of the measured response acceleration in the time period of confirmed variation of acceleration when the probe climber passed through damage area. Then, the specimens whose damage depths are 0, 0.9, 1.5 and 1.8, respectively, were compiled in the histogram shown in Figure 9.11, up to 20 Hz measured as the primary frequency band of response vibration.

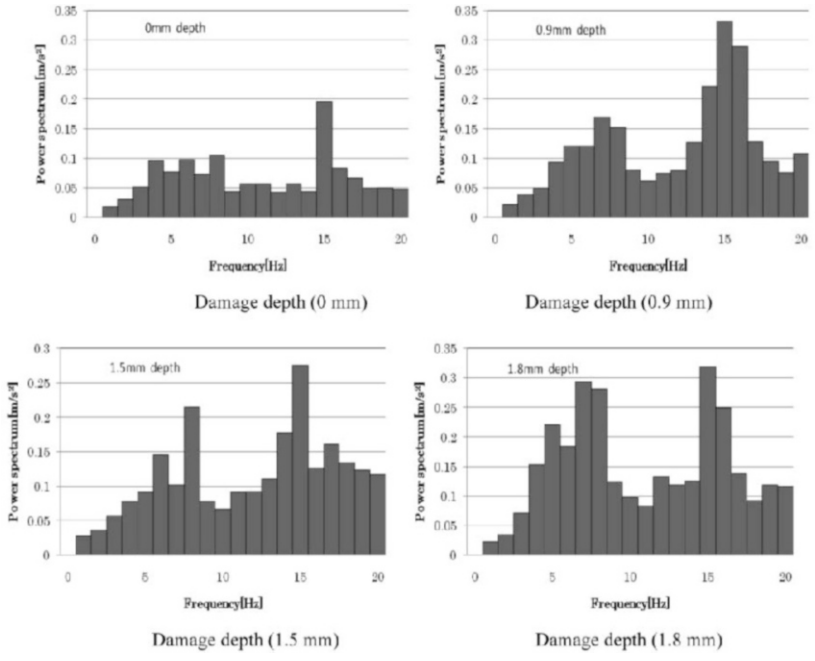

Figure 9.11. *Frequency response property*

In Figure 9.11, in each frequency up to 20 Hz, marked acceleration change caused by damage is confirmed in 5–8 Hz. In addition to this, large-scale power spectrum can be seen in the vicinity of 15 Hz, which, however, shows less change caused by damage depths. When compared with motor vibration data alone, it was confirmed that the power spectrum components came from vibrations of the probe climber's drive motor. Therefore, damage can be detected if attention is paid to acceleration changes in 5–8 Hz.

Next, in order to locate the occurrence of damage, time resolutions for measured signals are also important. Hence, signal processing was performed, using the wavelet transform that can ensure accuracy in both frequency resolution and time resolution. Figure 9.12 provides a comparison by the presence or absence of damage, regarding the results of the wavelet transform in the 4–8 Hz band, where the marked change was confirmed by the DFT applied to the response acceleration. It can be seen that the spectral intensity is remarkably greater in the right circle area in the lower part of Figure 9.13. When wire breakages were present above a certain level, response acceleration exceeding 0.2 m/s^2 could be detected in any of them. However, this integrity evaluation can be used only in the case of uniform motion. Even during the acceleration/deceleration of the automatic measuring device, response acceleration exceeds the threshold value as shown in the left circle in the lower part of Figure 9.12. This presents a possibility that response vibration caused by damage will be buried by the effects of acceleration/deceleration of the climber.

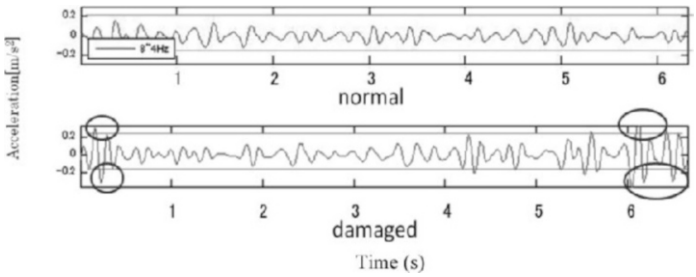

Figure 9.12. *Wavelet transeform signal for the response vibration*

9.6. Integrity evaluation of wire rope through MFL strength

Currently, an MFL measuring device of induction coil type is mainly used to detect wire breakages and rust on steel wire rope surfaces. As shown on the right side of Figure 9.13, this is a sensor system to detect small MFL

occurring in the areas of wire breakages and corrosion after a magnetizer organizes the magnetic lines of the wire rope, enabling checking of clear variations in MFL strength where slight damage or rust has occurred as shown in Figure 9.10.

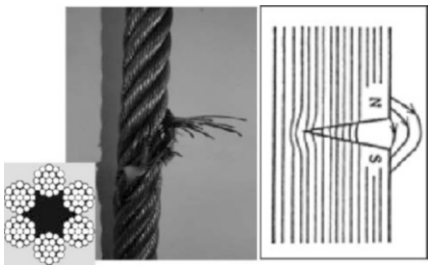

Figure 9.13. *Breakage of rope strand and leakage flux*

Figure 9.14 shows the result of wavelet transform applied to the MFL measurement data. Spectral variations can be also confirmed in the original waveform to the extent that damage can be detected. Then, Figure 9.15 provides the measurement results of the wire rope MFL strength in the number of wire breakages (0–5) equivalent to the initial damage, in order to examine the relationship between the MFL strength and the number of wire breakages.

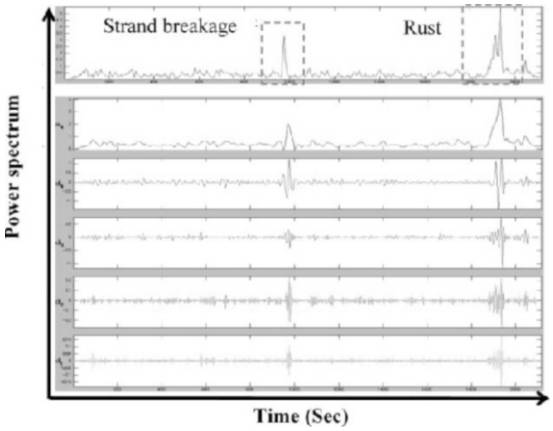

Figure 9.14. *Wavelet transform signal of the leakage flux*

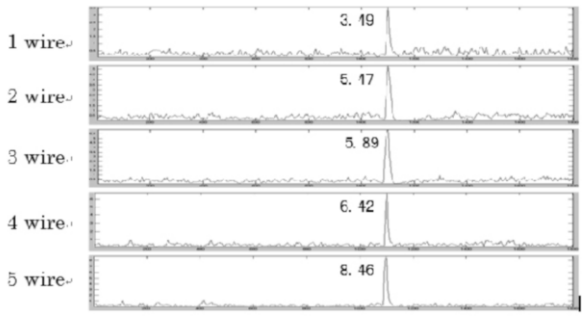

Figure 9.15. *Leakage flux for the number of strand breakages*

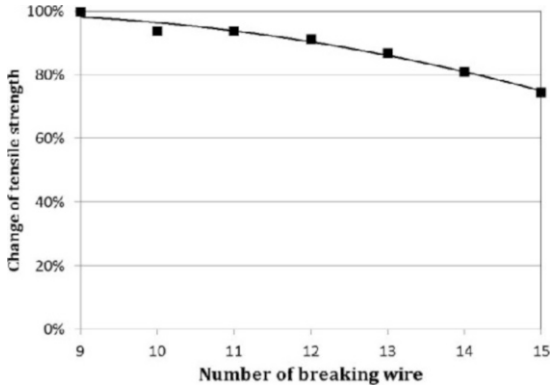

Figure 9.16. *Effects of the tensile strength to the number of breaking wires*

The results indicate that the MFL strength increases in proportion to the number of broken wires, which raises the possibility of estimating the number of initial external wire breakages. Subsequently, in order to verify the relationship between MFL strength and wire rope strength, a tensile test was conducted for wire rope with wire breakages and changes in tensile breaking strength were verified. Figure 9.17 shows the relationship between the number of wire breakages and the wire rope breaking strength in one strand of the wire rope (24 wires). In the range of the initial damage (about one–five wire breakages), there was virtually no decrease in the tensile strength. However, as the number of wire breakages approached 10, the tensile strength gradually decreased and it was observed that the wire rope strength was reduced by 10% or so, when 12 wires broke. Furthermore, in 12–15

breakages, a roughly linearly proportional decrease in the tensile strength was shown and 20% decrease in strength was observed in 14 wire breakages.

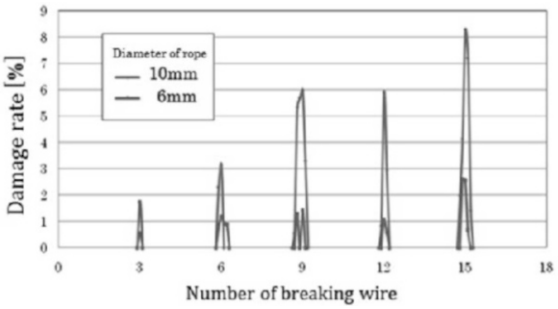

Figure 9.17. *Effects of damage rate to the diameter of wire rope and the number of breaking wires*

From the above discussion, an MFL measuring device of an induction coil type is an effective sensor system for detecting wire breakages, corrosion (rust) and wear on a wire rope surface. However, when it comes to handling the device, close attention is required to mount the device on the probe climber, as the device has a scanning speed limitation and is susceptible to the effects of vibrations. In addition, as shown in Figure 9.17, the device also has many demerits at present, such as decreased sensitivity in detecting small diameter wire rope and low accuracy in detecting inside wire breakages, such as in wire rope trough and bottom areas. Therefore, a sensor system was re-examined, which is light and compact, mountable on the probe climber and highly accurate in detecting damage. As an MFL detection method that has superior detection sensitivity for various forms of wire rope damage, a method using small Hall elements [SHA 12] can be considered, in addition to the induction coil type.

Hall elements were used because they have been conventionally considered difficult to use due to the temperature dependability but their recent developments have included III-V compound semiconductor InAs, which is highly sensitive and less temperature-dependent. As shown in Figure 9.18, a sensor system was built as a phased-array type that is reported to also enhance detection sensitivity. The phased-array Hall elements sensor prototyped in this study identifies relative damage positions and damage morphology from differences in respective response signals generated by a plurality of Hall elements arranged around the vicinity of the wire rope. This sensor, small and light, is also relatively easy to install into the probe climber.

The experiment conducted a comparative analysis of the cases of four and six Hall elements, respectively, and verified the effectiveness. Figure 9.19 shows the specimen onto which intensive wire breakages were provided on the wire rope surface. When the probe climber passed through this damage area, clear voltage changes could be detected in the Hall sensor system as shown in 9.19(b). From the above, the probe climber built in this study can detect damage and rust of wire rope, while elevating itself automatically. Its application to the automatic maintenance inspection of wire rope can be expected.

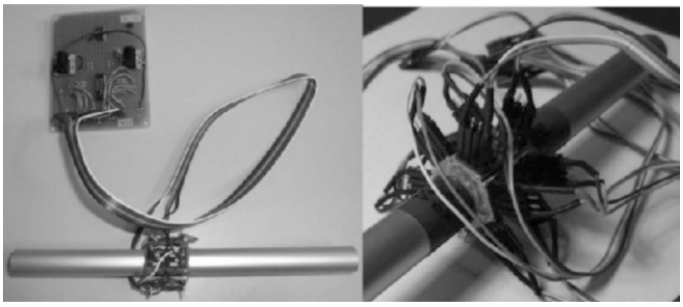

Figure 9.18. *Phased array hall sensor system*

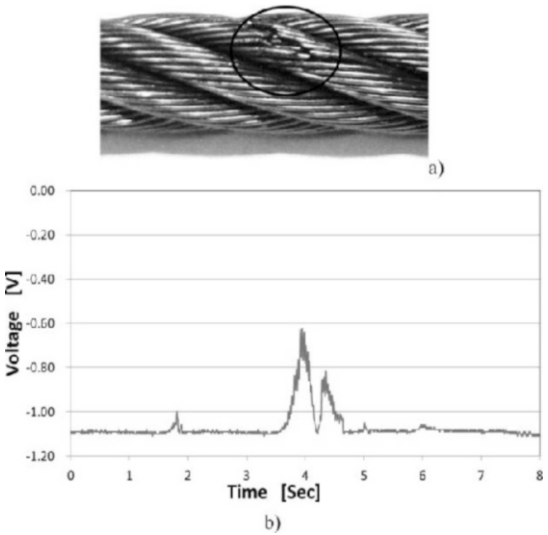

Figure 9.19. *Response signal of the phased-array Hall sensor system*

9.7. Damage detection of wire rope using neural networks

In the initial damage detection experiment for steel wire rope, the possibility was observed that MFL strength measured by the wire rope sensor could detect not only initial wire breakages but also rust occurrence areas. Then, damage detection using neural networks was tested in order to examine the possibility of automatic recognition by making the case analysis of wire breakages equivalent to the initial damage and rust occurrence. Table 9.4 indicates the output values by given measurement data and the estimated number of breakages after multilayer neural networks performed machine learning of 40 pieces of data on MFL strength (power spectrum) from initial wire breakages (zero–five breakages). The neural networks used for the machine learning were of a basic type with 10 hidden neurons, which has a two-layer structure that outputs to the output layer the case analysis of wire breakages and rust occurrence as well as the number of wire breakages, when an input is made to the input layer on the amount of variation and the spread of variation of the MFL strength: these networks after the postlearning neural networks show that they can almost exactly estimate the number of the wire breakages.

Input data of maximum power spectrum at the damage locations	Estimated power spectrum at the damage locations	Estimated number of breaking wire
0.98	0.98	0
3.49	3.30	1
4.82	4.97	2
6.39	6.27	3
6.46	8.26	4
8.39	9.04	5

Table 9.4. *Damage detection for the breaking wire of steel wire rope by the neural network*

9.8. Conclusion

The developed probe climber, an automatic-driving type inspection device for automatically detecting wire breakages and rust occurrence on wire rope, was prototyped and its performance was evaluated. The improved probe climber that was fabricated demonstrated that it could safely operate during repeated outdoor elevation of more than 500 m. In addition, a sensor system of phased-array type Hall elements was fabricated. Using the MFL variations, the system detected the locations of wire breakages and rust occurrence in the

initial stage and it was verified that the use of neural networks enabled distinguishing between wire breakages and rust occurrence by their distinctive signals and estimating the number of the wire breakages.

9.9. Bibliography

[HAB 06] HABIB M.K., "Mechatronics engineering the evolution, the needs and the challenges", *Proceedings of the 32nd Annual Conference of IEEE Industrial Electronics Society (IECON 2006)*, pp. 4510–4515, 2006.

[HAB 07] HABIB M.K., "Real time mapping and dynamic navigation for mobile robots", *International Journal of Advanced Robotic Systems*, vol. 4, no. 3, pp. 323–338, 2007.

[HAB 08] HABIB M.K., "Interdisciplinary mechatronics: problem solving, creative thinking and concurrent design dynergy", *International Journal of Mechatronics and Manufacturing Systems*, IEEE Industrial Electronics Society, vol. 1, no. 1, pp. 264–269, 2008.

[HAR 12] HARA E. *et al*., "Application to the cable maintenance system of the space elevator climber", *The Japan Society of Mechanical Engineers, Robotics and Mechatronics Conference 2012*, 1A2-L04, Japan, 28 May 2012.